Behavioral/Systems/Cognitive

Uncovering the Neural Signature of Lapsing Attention: Electrophysiological Signals Predict Errors up to 20 s before They Occur

Redmond G. O'Connell,[1,2] **Paul M. Dockree,**[1] **Ian H. Robertson,**[1] **Mark A. Bellgrove,**[2] **John J. Foxe,**[3,4] **and Simon P. Kelly**[3,4,5]

[1]School of Psychology and Trinity College Institute of Neuroscience, Trinity College Dublin, Dublin 2, Ireland, [2]School of Psychology and Queensland Brain Institute, University of Queensland, Brisbane, Queensland 4067, Australia, [3]The Cognitive Neurophysiology Laboratory, Nathan S. Kline Institute for Psychiatric Research, New York, New York 10962, [4]Program in Cognitive Neuroscience, Department of Psychology, City College of the City University of New York, New York, New York 10031, and [5]Center for Neurobiology and Behavior, Columbia University, New York, New York 10032

The extent to which changes in brain activity can foreshadow human error is uncertain yet has important theoretical and practical implications. The present study examined the temporal dynamics of electrocortical signals preceding a lapse of sustained attention. Twenty-one participants performed a continuous temporal expectancy task, which involved continuously monitoring a stream of regularly alternating patterned stimuli to detect a rarely occurring target stimulus whose duration was 40% longer. The stimulus stream flickered at a rate of 25 Hz to elicit a steady-state visual-evoked potential (SSVEP), which served as a continuous measure of basic visual processing. Increasing activity in the α band (8–14 Hz) was found beginning ~20 s before a missed target. This was followed by decreases in the amplitude of two event-related components over a short pretarget time frame: the frontal P3 (3–4 s) and contingent-negative variation (during the target interval). In contrast, SSVEP amplitude before hits and misses was closely matched, suggesting that the efficacy of ongoing basic visual processing was unaffected. Our results show that the specific neural signatures of attentional lapses are registered in the EEG up to 20 s before an error.

Introduction

The human capacity to sustain attention to behaviorally relevant stimuli is strongly challenged during highly routine task scenarios in which demands are low and external attention-grabbing events are few. Performance errors arising from transient inattention in real life can have catastrophic consequences, and an increased frequency of lapses characterizes a number of clinical syndromes, but our knowledge of their neural underpinnings remains limited.

The majority of EEG and functional magnetic resonance imaging (fMRI) studies have adopted block-design approaches that average across extended periods of behavior or event-related approaches that focus on the downstream consequences of attentional failures on transient target processing. The intertrial period before a target, when continuous attentional control is critical, has received far less investigation. Recently, Eichele et al. (2008) conducted a single-trial analysis of fMRI data and identified several patterns of hemodynamic activity that appeared to predict errors 6 s before they occurred with linear trends emerging up to 30 s beforehand. It remains to be seen whether such signatures are

detectable in more direct measures of cortical activity. EEG provides a high-temporal-resolution measure of postsynaptic cortical activity and represents an ideal technique for tracing the temporal evolution of maladaptive brain states. However, only a handful of studies to date have explored electrophysiological changes before a performance error, and their analyses have been limited to periods of just 1 or 2 s (Ridderinkhof et al., 2003; Allain et al., 2004; Hajcak et al., 2005). Adopting analysis strategies that can trace internally driven EEG changes over a broader timescale may prove fundamental to our understanding of the spatiotemporal evolution of attentional control.

Here, we report a comprehensive and systematic analysis of the psychophysiological precursors of lapses of sustained attention, defined here by the failure to detect a readily perceivable target stimulus, presented at fixation, during a novel continuous temporal monitoring task. First, we wished to establish how far back in time a lapse is foreshadowed in the EEG. To accurately gauge the timing of these error-predictive changes, EEG data were analyzed on three distinct timescales relative to the target: posttarget processing (+1 s), immediate pretarget processing (−4 s) and long-term pretarget processing (−30 s). Second, we sought to establish whether lapsing attention produces effects at all stages of stimulus processing, including "bottom-up" sensory processing or bears only on endogenous, higher-order processes. To provide a continuous measure of basic visual processing, task stimuli were presented at a 25-Hz flicker, thus eliciting a steady-state visual-evoked potential (SSVEP). By comparing SSVEP am-
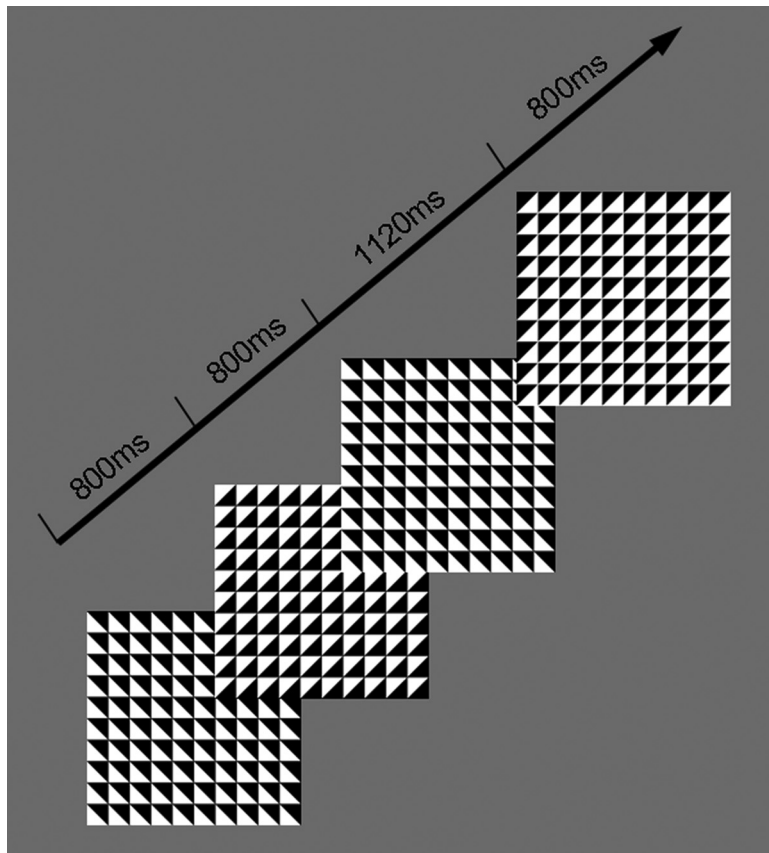
Figure 1. CTET. Participants monitored a continuous stream of patterned stimuli centrally presented and flickering at a rate of 25 Hz. Standard stimuli were presented for 800 ms, and participants were required to monitor for the occurrence of target stimuli defined by their longer duration (1120 ms) relative to other stimuli. Target detection was indicated by a speeded button press. All participants were practiced to a criterion level of performance.

plitude as well as early visual components of the transient event-related potentials (ERP) (Muller and Hillyard, 2000) within the 30 s preceding a hit/miss, we were able to assess the long-term effects of attentional lapses on bottom-up stimulus-evoked processes. Late higher-order transient ERP components and ongoing EEG rhythms were analyzed to explore the effects of lapsing attention on endogenous processes.

Materials and Methods

Participants
Twenty-nine participants volunteered for this experiment. One participant was excluded because that person was unable to consistently identify targets during practice, while seven were excluded because they made an insufficient number of hits or misses across all blocks (<20 after artifact removal) to generate reliable ERP averages, leaving a final sample of 21 participants (7 female, 3 left handed). All participants reported normal or corrected-to-normal vision and no current psychiatric diagnosis or history of head injury. All participants gave written informed consent, and all procedures were approved by the ethical review boards of the School of Psychology, Trinity College Dublin. Ethical guidelines were in accordance with the Declaration of Helsinki. Ages ranged from 19 to 31 years (mean, 25.67; SD, 2.53).

Continuous temporal expectancy task
In the continuous temporal expectancy task (CTET) (Fig. 1), a centrally presented patterned stimulus underwent a change at regular intervals, resulting in a continuous stream of "frames." The key requirement of the task was to monitor the temporal duration of each stimulus frame and to identify the minority of "target" frames with a duration that was 40% longer than the standard. The CTET was designed such that the temporal

judgments that were required were unchallenging when performed in isolation but demanding when participants were asked to continuously perform these judgments over an extended period. It was predicted that this task scenario would lead to more frequent lapses than the more common stimulus classification tasks that are used in attention research, thus facilitating EEG analysis. The pattern stimulus consisted of a single 8 cm² large square divided into a 10 × 10 grid of identical square tiles (0.8 mm²), each one diagonally split into black and white halves. The tile orientation shifted by 90° in a random direction (clockwise or counterclockwise) on each frame change yielding four distinct patterns. To reduce eye movement, participants were instructed to fixate on a white cross that was continuously presented at the center of the large square. All stimuli were presented on a gray background.

Standard (nontarget) stimuli were presented for 800 ms, and target stimuli were presented for 1120 ms. Stimuli were pseudo-randomly presented such that there were between 7 and 15 (average of 11) standard trials or 5.6–12 s (average 8.8 s) between each target presentation. To generate an SSVEP, the stimulus stream flickered on and off at a constant rate of 25 Hz. The SSVEP represents synchronous neuronal activity in early visual areas elicited by repetitive visual stimulation (Muller and Hillyard, 2000). Here, the SSVEP provided us with a continuous measure of basic visual stimulus processing. Participants were required to press a response key as quickly as possible when they detected a frame of longer duration (target). Each block consisted of 225 trials (frames) with a total duration of ∼3 min and 5 s. The number of targets varied between 18 and 22 per block. All participants completed 10 blocks of the task and were given a rest break in between each block.

To verify that the target/standard comparison was well above individual detection thresholds, all participants were required to exhibit 100% accuracy during an initial practice session. The practice session consisted of two separate practice blocks. In the first block, three targets were randomly interspersed among 25 standard stimuli. At this early stage, the stimuli were presented without the 25 Hz flicker to facilitate target identification. In the second practice block, an identical number of stimuli were presented, this time with the 25 Hz flicker. Participants were required to identify all target stimuli before advancing to the experimental trials. If participants missed one or more target stimuli, the practice was performed again. If the participant still failed to identify all the targets, they were excluded from the experiment. Only one participant was excluded on this basis, and they reported difficulty focusing on stimuli because of dry contact lenses. The duration of the target frame was made shorter (1060 ms) for one participant whose initial accuracy over the 10 blocks was close to ceiling (<20 errors in total). Hence, one participant performed the task twice, but only the data from the second attempt were analyzed.

Data analysis
Continuous EEG was acquired through the ActiveTwo Biosemi electrode system from 128 scalp electrodes, digitized at 512 Hz. Vertical eye movements were recorded with two vertical electrooculogram (EOG) electrodes placed below the left and right eye, while electrodes at the outer canthus of each eye recorded horizontal movements. Data were analyzed in Matlab R2007a. Data were re-referenced off-line to the nasion and low-pass filtered up to 40 Hz. All electrode channels were subjected to an artifact criterion of ±90 mV to reject trials with excessive EOG or other noise transients. To exclude errors that may have arisen from blinking

rather than true failures of attention, a 4 s window before each target trial was scanned, and any trial that included an artifact (±90 mV) that was evident across eight or more channels was excluded from all analyses. In all analyses of transient ERP, baseline and component intervals of a multiple of 40 ms were used, encapsulating an integer number of SSVEP cycles, to protect against contamination by residual SSVEP power remaining after notch-filtering.

The analysis proceeded in three stages: examining immediate target-related processing, short-term epochs preceding targets (4 s), and long-term epochs preceding targets (30 s). In all stages, we examined activity in a specific time interval relative to target trials (onset of longer-duration frame), comparing correctly detected trials (hits) to undetected trials (misses). For participants whose sweep count for hits versus misses was not matched, we randomly selected trials for inclusion from the overrepresented condition. It was also important to rule out the possibility that any differences between the two conditions could be attributed to a difference in the length of the average intertarget interval (ITI) associated with each condition. For example, previous work has demonstrated that the amplitude of the P3 component increases with ITI (Polich, 1990). Analysis of our own data in fact indicated that miss trials were associated with shorter ITI than hit trials (8.8 s vs 9.17 s; $t_{(20)} = 3.46$; $p < 0.01$). To control for this, random selection of trials in the overrepresented condition was carried out for each ITI separately, with the result that ITI of each length were equally represented in both conditions.

Immediate target processing. We examined the discrete event-related activity elicited by the detection of a target by deriving ERP for an epoch encapsulating the target interval (800–1120 ms) and beyond. A notch filter centered on 25 Hz was applied to eliminate the SSVEP activity in transient ERP. Stimulus-locked data were segmented into epochs of −100 ms before to 1800 ms after target frame onset and averaged separately for correctly detected targets and missed targets. Artifact rejection was based on a much broader preceding time frame starting from −3200, so that trials that were missed on account of preceding blinks or eye movement, as opposed to lapsing attention, were excluded. Target epochs were baseline corrected relative to the interval 560–640 ms, i.e., an 80 ms window centered on contingent negative variation (CNV) onset. The single subject for whom target frame duration was shorter was excluded from this analysis.

ERP component structure was confirmed by visual inspection of grand-average waveforms and associated scalp maps. The width of the latency window used to measure component amplitudes was based on the duration and spatial extent of each component. The target interval elicited the following components (Fig. 2): a strong negative shift over central scalp sites with onset ∼600 ms and peaking at 1000 ms (CNV) and a late positive wave with frontocentral (1200 ms; frontal target P3) and parietal maxima (1400 ms; parietal target P3).

We measured the CNV from a cluster of six electrodes centered on central (Cz) within the interval of 900–1100 ms (i.e., up until onset of the first posttarget standard frame). The late positive wave was measured around its dominant peak in the interval of 1300–1450 ms at both frontal and parietal sites. We tested for latency differences in the frontal target P3 by computing the onset and peak latency as follows: for each subject, we located the positive peak by finding the maximum within a window of 1120–1620 (or 0–500 ms relative to the transition from the target frame to the following standard). We then located the preceding "trough" as the minimum within a window extending from the beginning of the target interval (800 ms) to the positive peak just located. We defined the onset as that time point lying between the
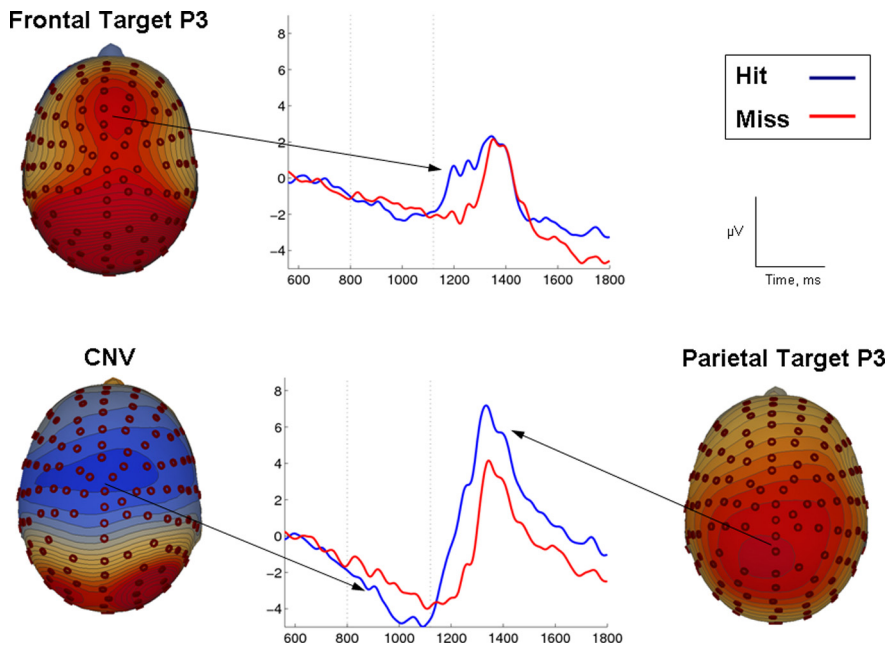

Figure 2. Immediate target processing. Grand average ERP waveforms and scalp topographies focused on the target detection interval and averaged separately for hits and misses. Scalp topographies show potential distribution for hits. Although the waveforms were time-locked to the onset of the target frame (time point 0), a target frame cannot be identified until its duration passes that of a standard frame (800–1120 ms, referred to as the target interval and highlighted by dashed vertical lines). The target interval elicited a central negativity between 600 and 1100 ms (CNV, bottom-left) and a late positive wave with fronto-central (1200 ms, frontal target P3; top) and parietal maxima (1400 ms, Parietal Target P3; bottom-right). Each of these components was reduced on miss trials.

trough and peak at which the potential rose above the trough level by 20% of the peak-trough difference.

Short-term pretarget processing. In the next step of our analysis, the goal was to look for divergences in electrophysiological markers within a relatively discrete time frame of 4 s. This window was selected to isolate activity that would be uncontaminated by the occurrence of other preceding target trials since the minimum intertarget interval was 5.6 s. For this time frame, we examined both the broadband transient ERP and spectral measures.

For the broadband ERP analysis, stimulus-locked data were segmented into epochs of −3200 ms before to 800 ms after target stimulus onset (i.e., until the beginning of the target interval). A notch filter of 25 Hz (width, 2 Hz) was applied to eliminate the SSVEP activity. Amplitude measures for the ERP components elicited by each of the four preceding standard frames and the target frame itself were acquired using separate baselines of −80 to 0 before the onset of each stimulus. Note that because a target frame cannot be identified as such until the 800 ms time point, we regarded it as the fifth pretarget standard frame here.

To select latency windows for the measurement of ERP components, a grand-average standard frame ERP was generated by averaging across the five frames preceding the target interval and without distinguishing between hits and misses (Fig. 3A). Standard frames elicited three principal ERP components: first, the early visual P1, maximal over occipital regions and peaking ∼120 ms after stimulus onset. Second, a frontal positivity, peaking at ∼300–350 ms. Finally, as in the target–interval waveform, we observed a CNV component with onset ∼600 ms and lasting until the following transient response. To reduce the likelihood that differences between detection conditions could be contaminated by activity differences at the prestimulus baseline, ERP component amplitudes were calculated by subtracting the amplitude at component onset from the peak amplitude (Table 1; Fig. 3A). Amplitude measures for each component were entered into a 2 × 5 ANOVA with two levels of detection (hit and miss) and five levels of trial (standard −4, standard −3, standard −2, standard −1, and target).

To measure effects on activity within discrete spectral bands, we used the Fast-Fourier transform to compute the amplitude spectrum across a
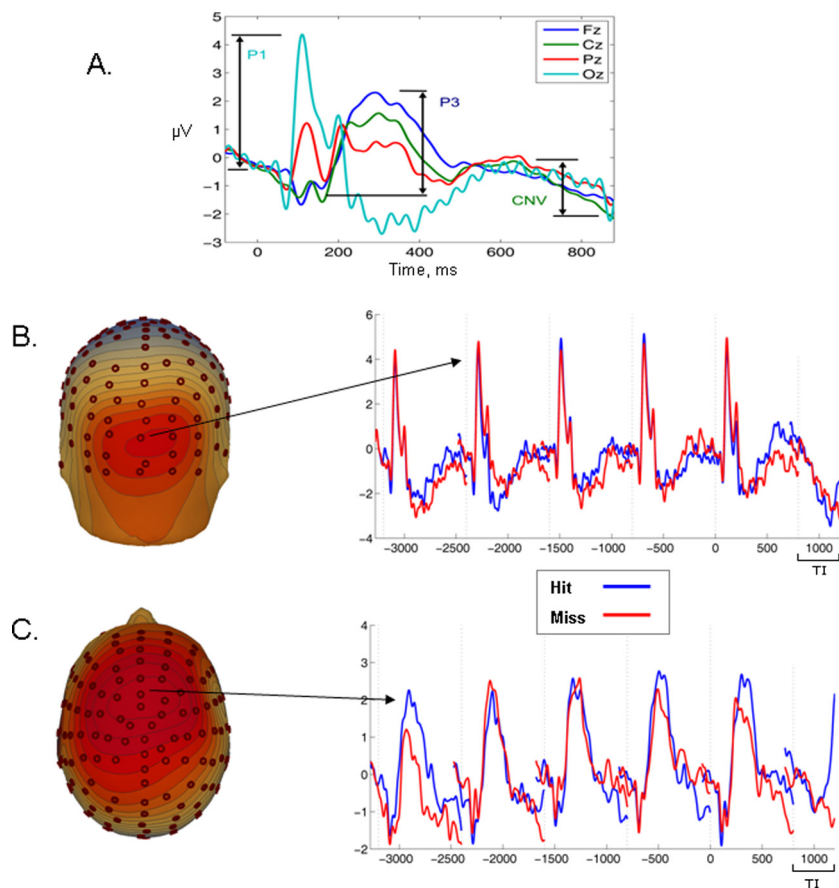
Figure 3. Short-term pretarget epoch. **A**, Grand-average ERP waveform for the five frames immediately preceding the target interval (TI) and collapsed across outcome. This waveform was used as the basis for defining component measurement intervals for the short- and long-term pretarget analysis. **B**, **C**, Grand-average ERP waveforms and associated scalp topographies within the epoch of −4000 ms pre-TI averaged separately according to subsequent target identification performance (hit, miss). Each stimulus change elicited a clear P1 response over visual areas (**B**), but its amplitude did not discriminate the two detection conditions, suggesting that basic visual processing was equated. In addition, each standard stimulus change elicited a strong P3 component over frontocentral scalp (**C**) that was increased before a hit relative to a miss.

Table 1. Latency intervals and electrode sites used for the measurement of ERP in the short-term pretarget epoch

Component	Onset interval (ms)	Peak interval (ms)	Electrodes
P1	−20 to 60	95–135	Nine electrodes surrounding Oz
Standard P3	80–160	280–400	Six electrodes surrounding Fz
CNV	560–640	760–840	Six electrodes surrounding Cz

4 s epoch extending from −3200 to +800 ms relative to target frame onset. Three dominant peaks were observed in grand average spectra collapsed across conditions: a relatively narrow spectral peak was identified within the theta band mainly over frontal sites; this was measured by integrating amplitude across the band 5–6.5 Hz. Alpha was measured in the broader standard band of 8–14 Hz, whereas SSVEP amplitude was measured at the discrete frequency of 25 Hz. Spectral amplitude measures were acquired individually from clusters of six electrodes centered on frontal (Fz), Cz, parietal (Pz), and occipital (Oz) scalp sites and entered into a 2 × 4 ANOVA with two levels of detection and four levels of region (frontal, central, parietal, and occipital). A separate ANOVA was carried out for each of the three bands.

Long-term pretarget processing. The next step in our analysis was designed to explore the longer-term temporal dynamics of the electrophysiological markers identified in the previous step and their relationship to performance on an upcoming target. On the basis of the findings of Eichele et al. (2008), we examined a 30 s long pretarget epoch. For the P3, we extracted an amplitude measure from each of 40 consecutive frames

ending on the target frame (starting 39 frames, or 31.2 s before target frame onset). P3 amplitude was computed as the integrated amplitude in the interval 280–400 ms minus that in the onset period from 80 to 160 ms relative to the onset of each frame (as in analysis step 2). Because of the rarity of 30 s periods of data that are free of blinks or other artifacts, we rejected a target trial only if an artifact was detected in the preceding 4 s using a 90 μV criterion as before. For all preceding frames, artifact rejection was carried out on a frame-by-frame basis. Because artifacts were distributed evenly across frames, this did not result in appreciably lower sweep counts for earlier frames than frames closer to the target. The average sweep count was in the range 42–49 for all frames. A smoothed series of 19 P3 amplitude measures, derived by averaging across windows of four frames in steps of 2, were entered into a 2 × 19 ANOVA with the factors of detection (hit vs miss) and time.

For the spectral measures of α and SSVEP, 2 s segments of data were extracted to provide reasonable frequency resolution. Starting with an epoch defined by the interval −1200 to 800 ms relative to target frame onset, we derived spectral measures at parietal and occipital sites for α (8–14 Hz) and SSVEP (25 Hz), respectively. We then proceeded in steps of two frames (1.6 s) back to 30 s before the target, resulting in 20 time points. To match the temporal smoothing applied to the P3, each pair of consecutive time bins was averaged, and a 2 × 19 ANOVA was carried out for each spectral measure, again with factors of detection and time. For the measures that showed an effect of detection in the short-term pretarget time frame, it was of interest to characterize the timing of the effect. Paired *t* tests were carried out for each of the 19 bins to determine the time bin at which each measure ceased to dissociate hits from misses. Given the exploratory nature of this step of the analysis, the more permissive cutoff of $p < 0.1$ was used to identify the time bins for which hit/miss divergences were strongest.

Results
Behavioral data
Participants completed 10 blocks of the CTET during which they were presented with an average of 200 target trials (range, 188–207). Over the 21 participants included in the analysis, 64% (SD, 15; range, 37–85) of target stimuli were correctly identified with an average reaction time of 626 ms (SD, 87; range, 510–922). The rate of false alarms was very low with an average of just 0.6% (SD, 0.6; range, 0–3), indicating that all participants were performing the task well above chance levels. We also examined performance accuracy as a function of time-on-task. Although performance did decline with time within block duration, $F_{(10,200)} = 13.5$, $p < 0.001$, there was no significant main effect of time-on-task across the 10 testing blocks, $F_{(9,198)} = 1.3$, $p = 0.2$ (see supplemental Fig. 1, available at www.jneurosci.org as supplemental material).

Immediate target processing
Since target stimuli are identical to standards, except for their increased duration, a target stimulus cannot be identified until its

duration has exceeded that of a standard. Therefore, in our analyses of the electrophysiological data, we made the distinction between "target onset," which is the time point at which the target frame begins (0 ms) and "target interval" (800–1120 ms), which is the window of time during which target identification is possible. All of the following analysis steps adhere to this convention whereby the zero time point corresponds to target frame onset.

Previous work has demonstrated that the amplitude of the CNV tends to increase with time, becoming more negative as an imperative stimulus approaches, consistent with a build-up of anticipatory activity (Macar and Vidal, 2004). On target trials in the CTET, we found that CNV amplitude continued to grow into the target interval (>800 ms) (Fig. 2) but to a much greater extent before a hit trial than a miss, $t_{(19)} = 2.87, p < 0.01$.

The late positive wave was measured around its dominant peak in the interval of 1300–1450 ms at both frontal and parietal sites. A 2×2 ANOVA with factors of region (frontal, parietal) and detection (hit, miss) revealed a main effect of detection, $F_{(1,19)} = 8.3, p < 0.05$, and a detection by region interaction, $F_{(1,19)} = 18.3, p < 0.001$. Comparing hits and misses at each region revealed a significant difference only at parietal sites ($p < 0.01$). Although target–P3 amplitude did not distinguish hits from misses at frontal sites in the time frame of its largest peak, a clear onset latency difference was evident at frontal sites (Fig. 2). We tested this by measuring the onset latency of the positive-going component at the frontal cluster of electrodes for hits and misses. The onset for hits (1057 ± 92 ms) was significantly earlier than the onset for misses (1154 ± 150 ms; $t_{(19)} = 4.24; p < 0.001$). It is also noted that the frontal target P3 onset was estimated to occur before the subsequent pattern change. Given the earliest reported onsets of purely stimulus-driven frontal scalp activity (Foxe and Simpson, 2002), it is clear that this positive deflection is not driven exogenously by the pattern shift itself in either condition. In fact, the peak latency of the frontal target P3 is ~300–400 ms after the point at which the next standard stimulus would have been expected to occur.

Short-term pretarget epoch
Divergences in electrophysiological markers were examined within a time-frame of 4 s before the onset of the target interval (Fig. 3).

Early sensory processing
The P1 was measured from a cluster of nine occipital electrodes surrounding occipital. No main effects were found (all $p > 0.4$).

Standard P3
For the standard P3, there was a significant main effect of detection, $F_{(1,20)} = 8.1, p < 0.01$, driven by larger amplitudes before correct target detections, but there was no main effect of trial ($p = 0.6$) and no trial by detection interaction ($p = 0.6$). Given the clear similarities between the scalp topographies and peak latencies, it is likely that the frontal target P3 (highlighted in
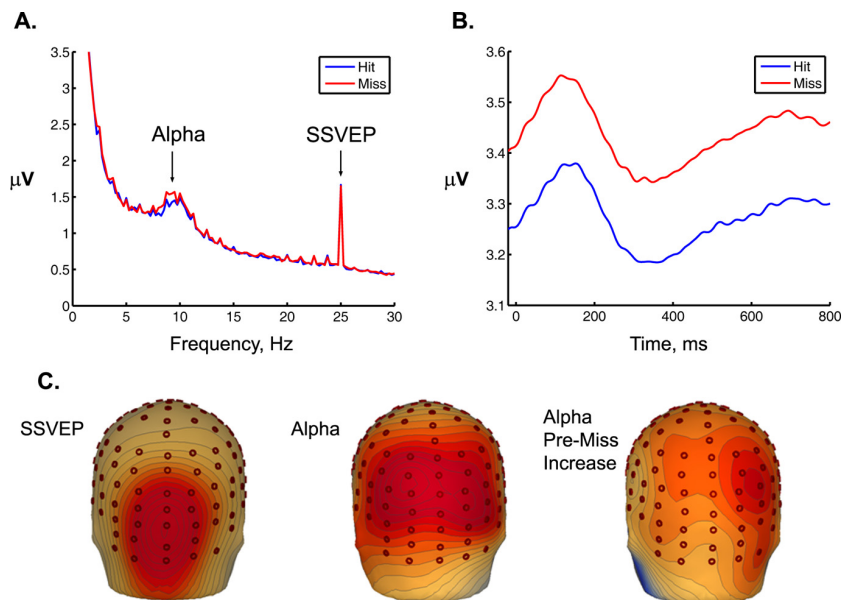

Figure 4. *A*, The continuous EEG amplitude spectrum calculated over occipital scalp sites for the 4 s period preceding a target. Amplitude differences before hits and misses are highlighted for α (8–14 Hz) and SSVEP (25 Hz). Relative to misses, hits were associated with reduced α before a target, but there were no differences in SSVEP amplitude, again suggesting that basic visual processing of the stimuli was matched across the two detection conditions. *B*, Grand-average temporal spectral evolution of α activity calculated for the five standard frames immediately preceding the target interval. The hit vs miss differential was evident across the entire epoch, and no systematic differences time-locked to stimulus onset were apparent. *C*, Scalp topographies for distribution of SSVEP and α activity as measured in the 4 s spectrum. The "SSVEP" and "alpha" topographies map spectral amplitude preceding hits. The "alpha pre-miss increase" topography was generated using a normalized measure [miss − hit]/[miss + hit]. The increase in α power before a miss was most prominent over right inferior parietal scalp sites and was clearly distinct from the central occipital SSVEP topography associated with basic visual processing.

analysis step 1) and standard P3 arise from the same endogenous processes that monitor the temporal structure of the task.

CNV
There were no significant main effects of time or detection for CNV amplitude (all $p > 0.3$).

EEG amplitude spectrum
The continuous EEG amplitude spectrum was also calculated for the 4 s pretarget epoch (Fig. 4).

Theta (5–6.5 Hz). There was no main effect of detection, $F_{(1,20)} = 1.3, p = 0.25$, but there was a main effect of region, $F_{(3,60)} = 4.1, p < 0.01$, and a detection by region interaction $F_{(3,60)} = 3.1, p < 0.05$. *Post hoc t* tests at each region indicated that theta amplitude did not reliably distinguish between hits and misses at any of the four scalp regions (all $p > 0.1$).

Alpha (8–14 Hz). There was a main effect of region, $F_{(3,60)} = 17, p < 0.001$, a marginal main effect of detection, $F_{(1,20)} = 3.8, p = 0.06$, and a significant detection by region interaction, $F_{(3,60)} = 4.9 p < 0.01$. *Post hoc t* tests at each region indicated significantly increased α amplitude before a miss relative to a hit, over parietal ($p < 0.05$) and occipital sites ($p < 0.05$), but not over central ($p = 0.1$) or frontal ($p = 0.2$) sites. To investigate whether the α-band effect had arisen from alterations in stimulus-evoked processing (e.g., visual-evoked components to the frame onset having power in the α band or differential α suppression in response to stimuli), we also examined the time course of α activity within the stimulus frames in the 4 s window. To this end, we derived temporal spectral evolution waveforms by filtering each 4 s epoch in the band 8–14 Hz, rectifying the filtered signals, smoothing with a 100 ms sliding window, and averaging across trials for each condition (Kelly et al. 2006; Thut
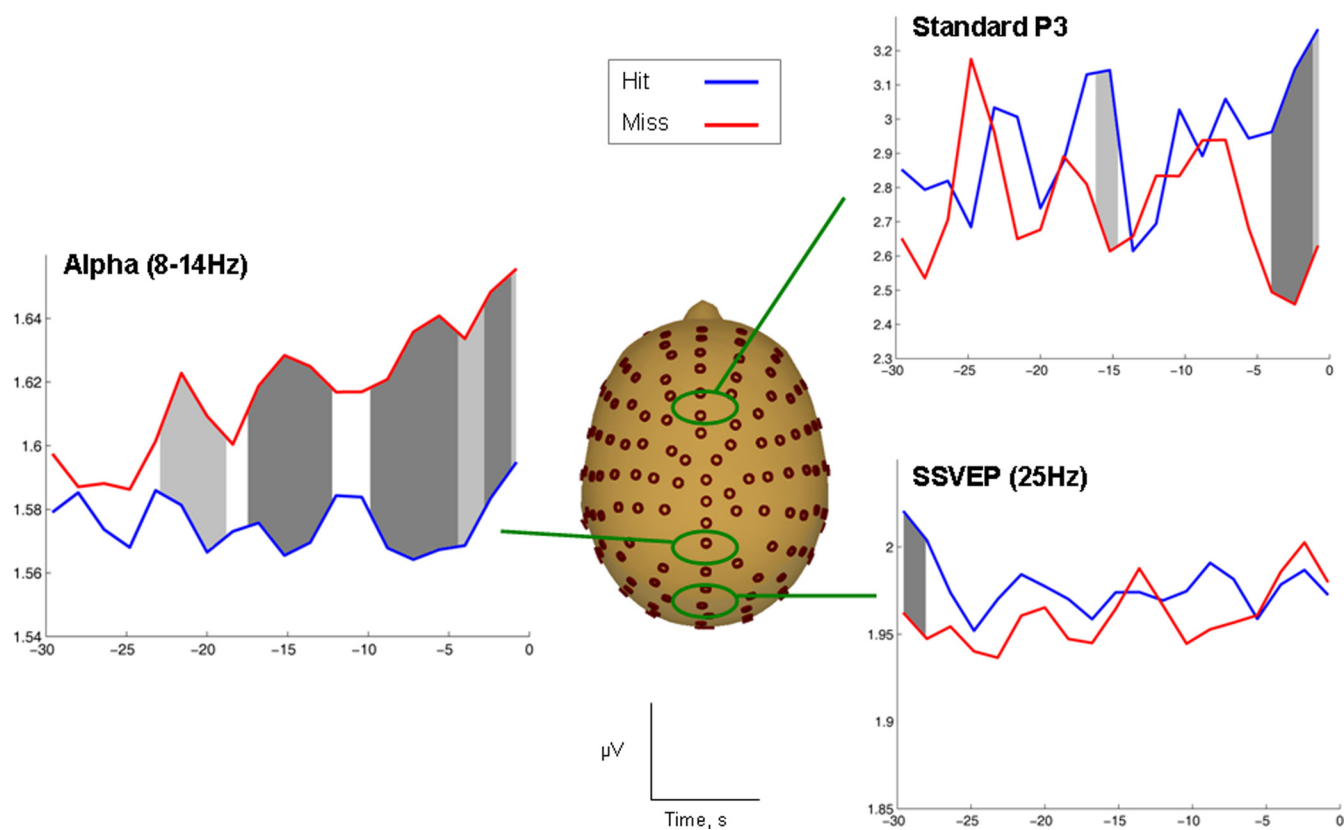
Figure 5. Long-term pretarget epoch. Standard P3, α, and SSVEP measures calculated over the 30 s period preceding target onset and averaged separately for hits and misses. No significant differences were found for SSVEP amplitude, but predictive differences were apparent for both α and frontal P3 over the 30 s epoch. Individual time-bin comparisons that reached significance are marked in gray (light gray denotes $p < 0.1$; dark gray denotes $p < 0.05$). For frontal P3 amplitude, the strongest differences were apparent 3–4 s before target onset. α-Band divergences were significant up to 20 s before an attentional lapse.

et al. 2006). Figure 4B shows the α time course in the epoch of 0–800 ms averaged across the five pretarget stimulus frames. No systematic differences time-locked to stimulus onset between hits and misses were apparent.

To examine the topography of the pre-error increase in α amplitude, we took a normalized measure of the difference, subtracting α before hits from α before misses and dividing by the sum of these conditions. Figure 4C shows the scalp distribution of this measure and, for comparison, the topographies of SSVEP amplitude and α amplitude for the hit condition. The increase in α power before a miss was most prominent over right inferior parietal scalp sites.

SSVEP (25 Hz). There was a significant main effect of region, $F_{(3,60)} = 21.7 \ p < 0.001$, reflecting stronger SSVEP amplitude over occipital regions, but there was no main effect of response ($p = 0.7$) and no detection by region interaction ($p = 0.3$). At the site of its overall maximum (cluster around occipital), SSVEP amplitude was 1.857 μV for hits and 1.858 μV for misses, indicating that basic sensory processing was closely matched.

Long-term pretarget epoch
The electrocortical markers that predicted successful target detection in the short-term epoch were then entered into a further analysis examining a 30 s period before the target interval (Fig. 5). On the basis of the results of analysis step 2, the standard P3 and parietal α amplitude were selected for further analysis. Although no differences were observed during the 4 s epoch, SSVEP amplitude was also selected for the analysis to account for any changes in visual cortical excitability preceding hits and misses.

Standard P3
For the standard P3, there was a strong trend toward an effect of detection, $F_{(1,20)} = 4.12$, $p = 0.056$, but no main effect of time, $F_{(18,360)} = 0.8$, $p = 0.6$, and no detection by time interaction ($p = 0.4$). To highlight the pretarget time point at which P3 amplitude ceased to distinguish between a subsequent hit or miss, a series of paired-samples t tests were conducted for each 4 s time bin. Differences appeared reliable only for the first three time bins (equivalent to 3–4 s) immediately before target frame onset (all $p < 0.1$).

Posterior alpha (8–14 Hz)
There were significant main effects of detection, $F_{(1,20)} = 5.53$, $p < 0.05$, and of time, $F_{(18,360)} = 2.7$, $p < 0.001$, and a detection by time interaction, $F_{(18,360)} = 2.2$, $p < 0.01$. Linear contrasts indicated that the interaction was driven by an increase in α over time before a miss ($p < 0.05$), whereas α amplitude remained stable before a hit ($p = 0.9$). Again, a series of paired-samples t tests were used as a means of exploring the time course of the α effect. Significant differences were evident for the last 14 of 19 total pretarget time points tested, i.e., the ~20 s immediately preceding a target in which α amplitude was significantly larger before a miss (all $p < 0.1$).

SSVEP (25 Hz)
There were no significant effects of trial or detection on SSVEP amplitude over the 30 s epoch (all $p > 0.1$). Time-bin comparisons also failed to identify any consistent divergences between the two detection conditions (hit, miss).

Discussion

The present study provides the first evidence that a lapse of sustained attention can be foreshadowed in electrophysiological signals up to 20 s before the occurrence of that lapse. Our data reveal specific maladaptive trends on multiple time-scales with slow drifts in α-band amplitude (20 s pretarget) followed by disruption of task-related time-monitoring mechanisms indexed by the P3 (3–4 s pretarget) and CNV (during target processing). These results indicate that relatively subtle behavioral changes can be anticipated ahead of time by monitoring changes in the EEG. The temporal trends identified here accord well with those of Eichele et al. (2008) and emphasize the important complimentary contributions of fMRI and EEG.

Sustained attention has been defined as the ability to maintain a mindful goal-directed focus in contexts whose repetitive, nonarousing qualities provide little external stimulation (Robertson and Garavan, 2004). Lapses of sustained attention are most likely to occur in highly routine and mundane task scenarios when we become prone to temporary goal neglect. The CTET paradigm was designed to test this ability by demanding the continuous deployment of attentional resources to the time domain. The ability to monitor time intervals is essential in guiding many everyday activities, and our subjective perception of the duration of stimuli is sharpened when attention is actively oriented to time (Nobre et al., 2007). This situation requires attention to be maintained more continuously over successive trials and thus places greater demands on top-down control resources than stimulus identification tasks such as the go/no-go, stop-signal, or flanker tasks in which classification can be concluded within the first few hundred milliseconds of presentation. An equally important aspect of this paradigm is that, aside from duration, the perceptual features of target and standard stimuli are identical. This bypasses the sometimes problematic issue of target salience automatically engaging attention and obviating the endogenous processes under investigation (Robertson and Garavan, 2004). Finally, that there was a strong decline in performance across just 3 min of task performance, but no broader decline over blocks indicates that the CTET is a useful paradigm for tracing drifts in the level of attentional control that are not related to changes in basal arousal levels.

α-Band activity provided the strongest electrophysiological predictor of a lapse of attention. Over the 30 s epoch, two distinct trends emerged: a maladaptive increase in activity, beginning ~20 s before a target and eventually leading to a behavioral lapse and an adaptive period of stable α levels associated with successful target detection. These differences were equally evident in the 4 s, target-free epoch, making it unlikely that the data are confounded by targets occurring within that interval. It is noteworthy that misses would not be consciously processed on the CTET since they result from the failure to detect a target. As such, the CTET would not entail a restoration of performance monitoring following errors as has been found on other tasks [e.g., the flanker task of Eichele et al. (2008)] and may thus provide a better estimation of the natural time course of attentional lapses unperturbed by evaluative error processing.

Activity in the α frequency band is thought to reflect the state of cortical excitability (Pfurtscheller, 2001). For example, studies that have focused on event-related synchronization (increase) and desynchronization (decrease) of α have pointed to antagonistic neural mechanisms that actively suppress and enhance visual cortical excitability when attention is deployed in space and time (Kelly et al., 2006; Thut et al., 2006; Romei et al., 2008a). Although the sensitivity of α activity to subtle changes in visual excitability has been well documented (Romei et al., 2008a,b), the α effects observed here are unlikely to reflect changes in baseline visual activity since we ob-

served no changes in either SSVEP or P1 amplitude, including on the target trial itself. The absence of any such relationship in our data is likely to be a product of the particular paradigm used. In contrast to previous α studies, most of which involved detection or discrimination tasks performed close to threshold levels (Thut et al., 2006; van Dijk et al., 2008), the CTET entails monitoring a centrally presented, high-contrast stream of continuous visual input that is well above detection thresholds. Moreover, it was verified that the increased duration of target frames was readily detectable at 100% accuracy during short practice runs. Consequently, performance is much less dependent on the active deployment of attention to the visual domain or the fine-tuning of perceptual thresholds. This made it possible to isolate "miss" trials that arose from a failure to sustain attention to stimulus duration as opposed to a temporary fluctuation in visual baseline activity.

Given that well-established indices of bottom-up visual stimulus processing (P1 and SSVEP) are unaffected, it would seem that the performance-predicting variance in α in our study is not the same marker of early visual cortical excitability as inferred in previous studies (Thut et al., 2006; Romei et al., 2008a,b; van Dijk et al., 2008). Numerous studies have demonstrated that early visual regions are not the only generators of α activity. Source analysis and combined EEG/fMRI studies have also mapped α activity in key nodes of the attentional control network, including the frontal and parietal cortices (Laufs et al., 2003, 2006; Moosmann et al., 2003; de Munck et al., 2007; Dockree et al., 2007). Although it is not possible to make strong claims regarding potential cortical generators on the basis of EEG topographies alone, the pre-miss α increase observed here was most strongly focused over right inferior parietal scalp and not over any of the regions that were associated with event-related stimulus processing. The right inferior parietal cortex has been heavily implicated in the top-down control of attention (Husain and Nachev, 2007), and the gradual increase in α amplitude appears consistent with the emergence of cortical idling or a resting state as controlled monitoring processes go off-line (Pfurtscheller and Lopes da Silva, 1999; Mantini et al., 2007). An alternative possibility is that this α trend arises from decreasing recruitment of specialized temporal processing regions. Transcranial magnetic stimulation and lesion studies have indicated that the right inferior parietal cortex also forms a critical part of the dorsal "when" pathway, which underpins our perception of time (Battelli et al., 2008; Van Rullen et al., 2008). The actual source of the present α trends may be best elucidated by combining EEG with brain imaging methods that provide fine-grained spatial resolution (e.g., fMRI) to explore the interaction of distributed functional networks.

The absence of any differences in visual perceptual analysis of task stimuli is consistent with previous reports that temporal expectation alone does not modulate the visual P1 component but specifically affects higher levels of stimulus processing relevant to goal monitoring and response execution as indexed by components such as the P3 and CNV (Miniussi et al., 1999; Doherty et al., 2005). An interesting avenue for future research may be to explore whether top-down modulation of the SSVEP emerges when participants are required to monitor for a visual feature such as a change in the frequency of the stimulus flicker.

The frontal P3 component differentiated hits from misses over both the long and short pretarget epochs. The analysis of the target trial for hits is revealing in that a component with the same temporal and topographical characteristics as the standard P3 was elicited during the additional target trial duration in the absence of any stimulus changeover. Previous studies of rhythm perception have pointed to a link between increased P3 amplitudes and improved timing (Jongsma et al., 2007; Correa and Nobre, 2008). The fact that a fron-

tal P3 was elicited during the target interval in the absence of a stimulus change indicates that this component is not stimulus driven but represents an active endogenous mechanism that traces the temporal structure of the task (Busse and Woldorff, 2003). Although amplitude differences reached significance across the 30 s epoch, no clear trends were apparent in the P3 signal that could differentiate the two detection conditions. The largest divergences occurred in the 3–4 s immediately preceding target onset, suggesting a brief disengagement of this monitoring mechanism immediately before a behavioral lapse.

The effect of an attentional lapse on the CNV appeared to be even more fleeting, with differences only apparent on the target trial itself. Previous research has demonstrated that the CNV represents the anticipatory deployment of attention before the presentation of an expected imperative stimulus as well as the preparation of an associated response (Miniussi et al., 1999; Brunia and van Boxtel, 2001). In the present study, the CNV grew in amplitude as the expected onset of the next stimulus approached, peaking at ~800 ms on standard frames but extending to 1100 ms on target trials. CNV amplitude was significantly attenuated on miss trials, indicative of a momentary reduction in target anticipation and consistent with the earlier disengagement of the P3 time-monitoring mechanism.

While top-down control gradually decays over the 20 s timescale, the shorter-term changes in the task-specific monitoring processes indexed by the standard P3 and CNV suggest that a critical threshold may need to be passed before task performance is actually compromised. This raises the interesting possibility that feedback on α-band states could be used as an early warning system to avert critical lapses of attention.

In conclusion, the present study reports a novel approach to the analysis of electrophysiological markers of lapsing attention that opens many new avenues for investigation. Our results identify maladaptive neural patterns operating on at least two distinct timescales: longer-term drifts in α amplitude (up to 20 s) preceding short-term disruption of performance-monitoring mechanisms before target onset (3–4 s). The absence of any change in early sensory processing indicates that lapsing top-down attention impacts primarily on higher-order endogenous mechanisms, at least in the present task scenario in which performance does not rely heavily upon perceptual acuity. Exploring prelapse activity may help to better characterize the neuropsychological deficits in a range of clinical groups and could contribute to the development of new rehabilitative techniques.

References

Allain S, Carbonnell L, Falkenstein M, Burle B, Vidal F (2004) The modulation of the Ne-like wave on correct responses foreshadows errors. Neurosci Lett 372:161–166.

Battelli L, Walsh V, Pascual-Leone A, Cavanagh P (2008) The "when" parietal pathway explored by lesion studies. Curr Opin Neurobiol 18:120–126.

Brunia CH, van Boxtel GJ (2001) Wait and see. Int J Psychophysiol 43:59–75.

Busse L, Woldorff MG (2003) The ERP omitted stimulus response to "no-stim" events and its implications for fast-rate event-related fMRI designs. Neuroimage 18:856–864.

Correa A, Nobre AC (2008) Neural modulation by regularity and passage of time. J Neurophysiol 100:1649–1655.

de Munck JC, Gonçalves SI, Huijboom L, Kuijer JP, Pouwels PJ, Heethaar RM, Lopes da Silva FH (2007) The hemodynamic response of the alpha rhythm: an EEG/fMRI study. Neuroimage 15:1142–1151.

Dockree PM, Kelly SP, Foxe JJ, Reilly RB, Robertson IH (2007) Optimal sustained attention is linked to the spectral content of background EEG activity: greater ongoing tonic alpha (approximately 10 Hz) power supports successful phasic goal activation. Eur J Neurosci 25:900–907.

Doherty JR, Rao A, Mesulam MM, Nobre AC (2005) Synergistic effect of combined temporal and spatial expectations on visual attention. J Neurosci 25:8259–8266.

Eichele T, Debener S, Calhoun VD, Specht K, Engel AK, Hugdahl K, von Cramon DY, Ullsperger M (2008) Prediction of human errors by maladaptive changes in event-related brain networks. Proc Natl Acad Sci U S A 105:6173–6178.

Foxe JJ, Simpson GV (2002) Flow of activation from V1 to frontal cortex in humans: a framework for defining "early" visual processing. Exp Brain Res 142:139–150.

Hajcak G, Nieuwenhuis S, Ridderinkhof KR, Simons RF (2005) Error-preceding brain activity: robustness, temporal dynamics and boundary conditions. Biol Psychol 70:67–78.

Husain M, Nachev P (2007) Space and the parietal cortex. Trends Cogn Sci 11:30–36.

Jongsma ML, Meeuwissen E, Vos PG, Maes R (2007) Rhythm perception: speeding up or slowing down affects different subcomponents of the ERP P3 complex. Biol Psychol 75:219–228.

Kelly SP, Lalor EC, Reilly RB, Foxe JJ (2006) Increases in alpha oscillatory power reflect an active retinotopic mechanism for distracter suppression during sustained visuospatial attention. J Neurophysiol 95:3844–3851.

Laufs H, Kleinschmidt A, Beyerle A, Eger E, Salek-Haddadi A, Preibisch C, Krakow K (2003) EEG-correlated fMRI of human alpha activity. Neuroimage 19:1463–1476.

Laufs H, Holt JL, Elfont R, Krams M, Paul JS, Krakow K, Kleinschmidt A (2006) Where the BOLD signal goes when alpha EEG leaves. Neuroimage 31:1408–1418.

Macar F, Vidal F (2004) Event-related potentials as indices of time processing: a review. J Psychophysiol 18:89–104.

Mantini D, Perrucci MG, Del Gratta C, Romani GL, Corbetta M (2007) Electrophysiological signatures of resting state networks in the human brain. Proc Natl Acad Sci U S A 104:13170–13175.

Miniussi C, Wilding EL, Coull JT, Nobre AC (1999) Orienting attention in time. Modulation of brain potentials. Brain 122:1507–1518.

Moosmann M, Ritter P, Krastel I, Brink A, Thees S, Blankenburg F, Taskin B, Obrig H, Villringer A (2003) Correlates of alpha rhythm in functional magnetic resonance imaging and near infrared spectroscopy. Neuroimage 20:145–158.

Müller MM, Hillyard S (2000) Concurrent recording of steady-state and transient event-related potentials as indices of visual-spatial selective attention. Clin Neurophysiol 111:1544–1552.

Nobre A, Correa A, Coull J (2007) The hazards of time. Curr Opin Neurobiol 17:465–470.

Pfurtscheller G (2001) Functional brain imaging based on ERD/ERS. Vision Res 41:1257–1260.

Pfurtscheller G, Lopes da Silva FH (1999) Event-related EEG/MEG synchronization and desynchronization: basic principles. Clin Neurophysiol 110:1842–1857.

Polich J (1990) Probability and interstimulus interval effects on the P300 from auditory stimuli. Int J Psychophysiol 10:163–170.

Ridderinkhof KR, Nieuwenhuis S, Bashore TR (2003) Errors are foreshadowed in brain potentials associated with action monitoring in cingulate cortex in humans. Neurosci Lett 348:1–4.

Robertson IH, Garavan H (2004) Vigilant attention. In: The cognitive neurosciences, Ed 3 (Gazzaniga MS, ed), pp 631–640. Cambridge, MA: MIT.

Romei V, Rihs T, Brodbeck V, Thut G (2008a) Resting electroencephalogram alpha-power over posterior sites indexes baseline visual cortex excitability. Neuroreport 19:203–208.

Romei V, Brodbeck V, Michel C, Amedi A, Pascual-Leone A, Thut G (2008b) Spontaneous fluctuations in posterior alpha-band EEG activity reflect variability in excitability of human visual areas. Cereb Cortex 18:2010–2018.

Thut G, Nietzel A, Brandt SA, Pascual-Leone A (2006) α-Band electroencephalographic activity over occipital cortex indexes visuospatial attention bias and predicts visual target detection. J Neurosci 26:9494–9502.

van Dijk H, Schoffelen JM, Oostenveld R, Jensen O (2008) Prestimulus oscillatory activity in the alpha band predicts visual discrimination ability. J Neurosci 28:1816–1823.

VanRullen R, Pascual-Leone A, Battelli L (2008) The continuous Wagon wheel illusion and the "when" pathway of the right parietal lobe: a repetitive transcranial magnetic stimulation study. PLoS ONE 3:e2911.